Journal of Neonatal Surgery
ISSN(Online): 2226-0439
Vol. 13, (2024)
https://www.jneonatalsurg.com

OPEN ACCESS

Spectroscopic Investigation of Protein Binding and Antibacterial Activity in Hybrid CuO–Bi(III) Schiff Base Complexes

S. Rama pandian[1,2], A. Mathavan[*2], C. Vedhi[*2]

[1]Research Scholar, Registration Number: 17232232031011, V. O. Chidambaram College, Tuticorin - 628 008 (affiliated) Manonmaniam Sundaranar University, Abishekapatti, Tirunelveli, Tamil Nadu 627 012, India

[2]Department of Chemistry, V. O. Chidambaram College, Tuticorin 628 008, Tamil Nadu, India

***Corresponding Author:**

Email ID: abhimathavan@gmail.com

Email ID: cvedhi23@gmail.com

Cite this paper as: S. Rama pandian, A. Mathavan, C. Vedhi, (2024) Spectroscopic Investigation of Protein Binding and Antibacterial Activity in Hybrid CuO–Bi(III) Schiff Base Complexes. *Journal of Neonatal Surgery*, 13, 662-672.

ABSTRACT

This study presents the development and characterization of hybrid CuO–Bi(III) Schiff base nanocomposites. Copper oxide nanoparticles were synthesized via a simple precipitation method and functionalized with a salen ligand and a bismuth-salen complex, forming CuO–Salen and CuO–SBC. Spectroscopic analyses (FT-IR, UV-Vis) confirmed successful coordination, with characteristic Cu–O bands and LMCT absorption up to 700 nm. The optical band gap reduced from 2.27 eV (CuO) to 1.99 eV (CuO–SBC), indicating enhanced charge transfer. FE-SEM showed a porous structure, and XRD confirmed nanoscale crystallinity. Binding studies with BSA and HSA revealed strong interactions, especially for CuO–SBC (Ka: 1.2×10^5 M^{-1} and 3.5×10^5 M^{-1}). Antibacterial tests showed CuO–SBC had the highest activity, with a 19 mm inhibition zone against *Bacillus subtilis*. Overall, CuO–SBC demonstrated excellent biological activity, highlighting its potential in drug delivery and antimicrobial applications.

Keywords: *Schiff base complexes, Bismuth (III), CuO hybrids, Optical properties, Protein binding, Antibacterial activity.*

1. INTRODUCTION

Copper oxide (CuO) nanoparticles have drawn considerable interest in nanomedicine and materials science for their excellent electronic, catalytic, and antimicrobial properties [1, 2]. Their narrow band gap, high surface area, and ability to generate reactive oxygen species make them ideal for antibacterial and biochemical applications [3, 4]. Combining CuO with Schiff base ligands particularly salen-type compounds derived from salicylaldehyde and ethylenediamine enhances their biological potential. These ligands are known for strong metal binding, biocompatibility, and the ability to form stable, redox-active complexes with transition metals [5–8]. Such hybrid materials often outperform their individual components in bioactivity and binding efficiency [9, 10]. Bismuth(III)-based Schiff base complexes (SBCs) further elevate functionality by offering excellent coordination stability, low toxicity, and broad-spectrum antimicrobial effects with minimal resistance [11, 12]. In this study, CuO–Salen and CuO–SBC nanocomposites were synthesized and analyzed for their structural, optical, and biological properties. Given the rising demand for effective bio-interactive and antimicrobial agents, we focused on their protein-binding behavior with model proteins bovine and human serum albumins (BSA and HSA) and antibacterial performance against Gram-positive and Gram-negative bacteria [13–16]. This work highlights the potential of these multifunctional nanocomposites for biomedical applications, particularly in drug delivery and antimicrobial therapy.

2. MATERIAL AND METHODOLOGY

Materials:

All chemicals used were of analytical grade and used without further purification. Copper(II) sulfate pentahydrate ($CuSO_4 \cdot 5H_2O$), sodium hydroxide (NaOH), salicylaldehyde, ethylenediamine, and bismuth nitrate were purchased from commercial suppliers. Distilled water was used throughout the synthesis process.

Synthesis of Copper Oxide (CuO) Nanoparticles

CuO nanoparticles were synthesized via a straightforward precipitation method. In a 250 mL round-bottom flask, 0.624 g (0.01 M) of $CuSO_4$ was dissolved in distilled water, and 1 g of NaOH pellets was slowly added under constant stirring. The mixture was stirred for 2 hours, during which the color changed from blue to black, indicating CuO formation. The black precipitate was filtered, washed, and calcined at 400 °C for 1 hour.

Preparation of CuO–Salen Nanocomposite

To prepare the CuO–Salen nanocomposite, the synthesized CuO was dispersed in a basic medium (NaOH or NH_4OH), followed by the addition of Salen ligand in a 1:1 molar ratio. The mixture was stirred until a black gel formed, then centrifuged at 100 rpm and dried to obtain the CuO–Salen composite.

Preparation of CuO–SBC Nanocomposite

For the CuO–SBC nanocomposite, CuO was suspended in NaOH or NH_4OH and mixed with an equal amount of Bismuth Salen complex (SBC) in a 1:1 ratio. A grey gel formed, which was calcined at 120 °C, centrifuged at 100 rpm, and dried to yield the CuO–SBC composite.

Characterization

The FT-IR spectra were recorded using a computer-controlled Thermofisher scientific instrument. A computer-controlled JASCO V-530 and FP-8300 was used to study UV-VIS spectral and fluorescence behavior. XRD measurements were made by Panalytical X'Pert Powder X'Celerator Diffractometer, measurement range: 10 to 80 degrees in 2θ and particle size was calculated using Scherrer's equation. The FESEM measurements were carried out by JEOL JSM-6700F field emission scanning electron microscope.

3. RESULTS AND DISCUSSION

FT-IR Studies

The FT-IR spectra of CuO, the Bi–Salen complex, and the CuO–Bi–Salen composite (Figure 1) reveal important details about their functional groups and coordination interactions. The CuO spectrum (Figure 1a) shows characteristic Cu–O stretching bands in the 500–600 cm^{-1} range, confirming the presence of copper oxide, consistent with earlier reports [18]. In the CuO–Salen spectrum (Figure 1b), shifts in the C=N stretching band suggest coordination between CuO and the salen ligand. New peaks in the 500–600 cm^{-1} region correspond to Cu–N and Cu–O bonds, supporting successful complex formation [18]. The CuO–Bi–Salen spectrum (Figure 1c) also shows a shifted C=N band relative to the free Bi–Salen ligand, indicating imine-metal coordination [17]. Additional peaks in the Cu–N and Cu–O regions confirm the formation of the CuO–Bi–Salen complex. The spectral shifts and new vibrational bands confirm strong coordination between CuO and the ligands, validating the successful synthesis of the nanocomposites. These findings align with previous studies on metal–Schiff base complexes [19].

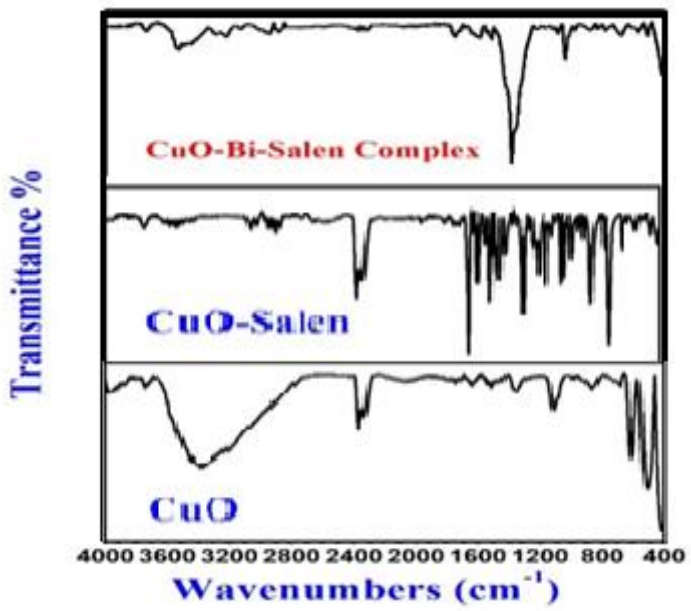

Fig.1. FT-IR Spectrum of a) CuO b) CuO- salen complex c) CuO-Bi-Salen complex

UV-Vis Studies

The UV–Vis spectra of CuO, CuO–Salen, and CuO–Bi–Salen (Figure 2) reveal distinct absorption shifts due to ligand coordination. Pure CuO shows a broad band around 280–320 nm, corresponding to $O^{2-} \rightarrow Cu^{2+}$ charge transfer transitions [24, 25]. Upon complexation with Salen, new peaks appear in the 300–350 nm and 500–700 nm ranges. These are attributed to π–π* transitions of the Salen ligand and ligand-to-metal charge transfer (LMCT), confirming strong Cu–ligand interactions [20, 21]. In the CuO–Bi–Salen complex, absorption extends further into the visible region, indicating enhanced charge transfer and improved electronic coupling due to Bi(III) incorporation [22, 23]. This red shift also suggests improved light-harvesting potential, relevant for photocatalysis and optoelectronics. The optical band gaps, calculated from Tauc plots (Figure 3), further support these observations. Pure CuO exhibited a band gap of 2.27 eV, which decreased to 2.19 eV for CuO–Salen and to 1.99 eV for CuO–Bi–Salen. This progressive narrowing of the band gap reflects better electronic delocalization and stronger metal–ligand interactions, especially with bismuth. Such tunable optical properties make these materials promising for applications in solar energy conversion, sensing, and photocatalytic systems [26, 27].

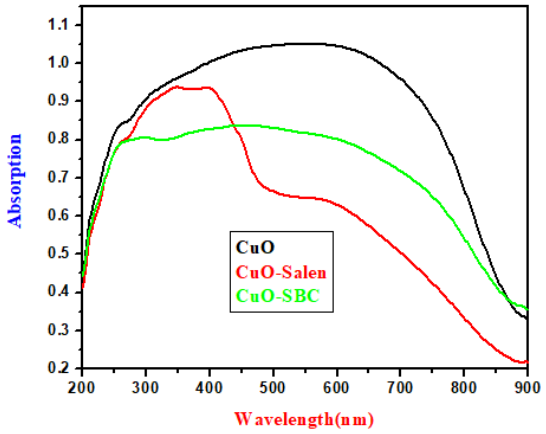

Fig.2. UV-Vis Spectrum of a) CuO b) CuO-salen complex c) CuO-Bi-Salen complex

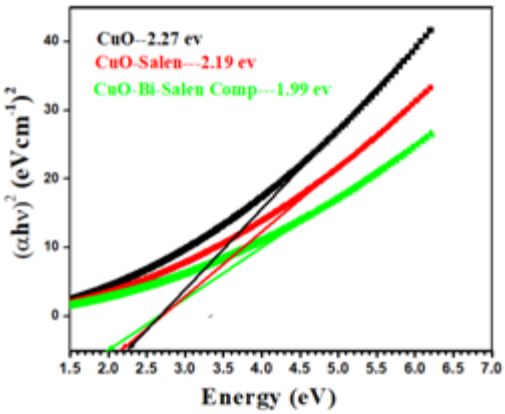

Fig 3. Band gap curve of a) CuO b) CuO-salen complex c) CuO-Bi-Salen complex

FE-SEM Studies

The FE-SEM image of CuO (Fig. 4) shows a porous, irregular surface with nanoscale agglomerates, indicating high surface area ideal for catalysis and gas sensing [28–30]. It's rough texture and loose packing enhance active site availability and ion diffusion, supporting potential electrochemical applications [31]. In CuO–Bi–Salen (Fig. 5), the structure remains porous and agglomerated, with irregular nanoparticles suggesting strong metal–ligand interaction. The increased surface roughness and nanoscale features improve catalytic and sensing performance [22, 22, 32], consistent with reported hybrid metal-organic systems.

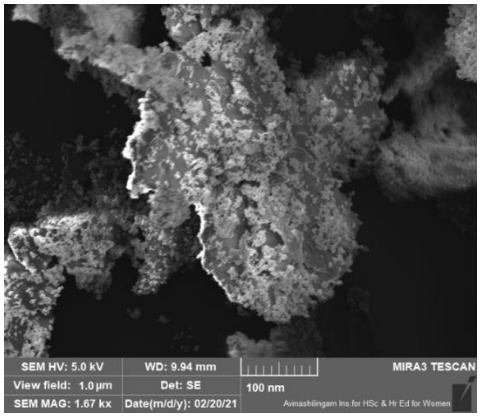

Fig.4. FE-SEM image of CuO

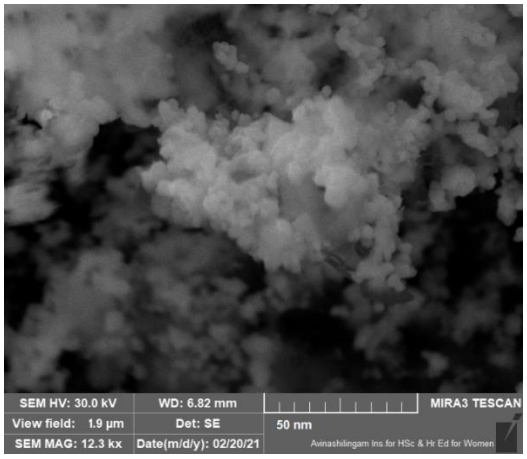

Fig.5. FE-SEM image of CuO-Bi-Salen Complex

XRD Studies

XRD patterns confirmed the crystalline nature and phase identity of the synthesized materials. For CuO (Fig. 6), sharp peaks at 2θ = 35.5°, 38.7°, 48.7°, 58.3°, and 68.1° match monoclinic CuO (JCPDS No. 48-1548), with a calculated crystallite size of 8.4 nm. The CuO–Salen complex (Fig. 7) showed reduced CuO peak intensity and new reflections at 24.6° and 28.4°, indicating ligand coordination [33]. The estimated crystallite size was 16.2 nm. CuO–Bi–Salen (Fig. 8) displayed a broad peak near 28°, suggesting low crystallinity and nanoscale features. The crystallite size was 10.2 nm. Minor shifts and broadening imply Bi coordination, consistent with Bi-based complexes (JCPDS No. 05-0519) [34]. These results confirm successful complex formation and ligand-induced structural modifications.

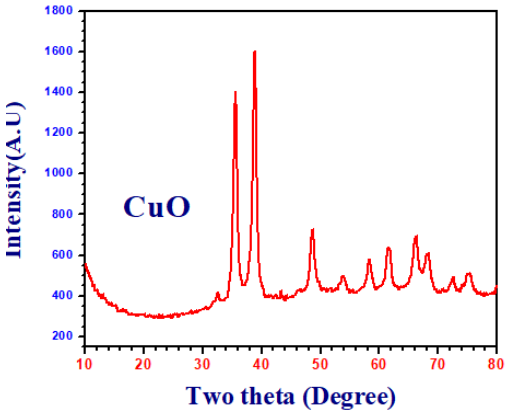

Fig.6. XRD image of CuO

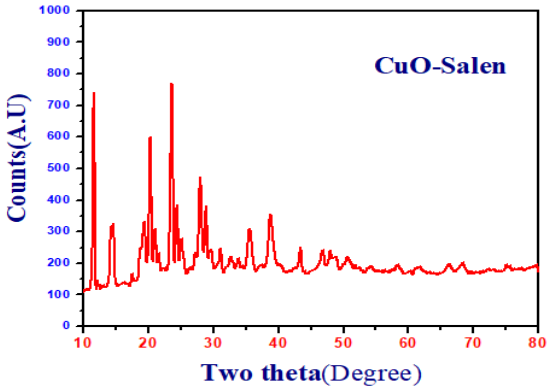

Fig.7. XRD image of CuO-Salen Complex

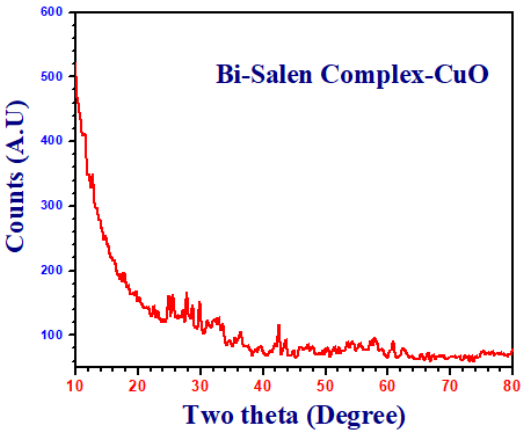

Fig.8. XRD image of CuO-Bi-Salen Complex

Binding Studies of Bovine Serum Albumin (BSA) with Different Complexes

The binding behavior of BSA with CuO-based complexes was evaluated using fluorescence quenching and UV–Vis spectroscopy to assess their suitability for biomedical applications. In Figure 9a and 9b, CuO nanoparticles showed a noticeable decrease in BSA fluorescence, indicating moderate binding. The Stern–Volmer constant (K_{SV}) was $3.5 \times 10^4\ M^{-1}$, suggesting static quenching and formation of a CuO–BSA complex, likely involving coordination and hydrophobic interactions [35]. Figure 10a and 10b show that the CuO–Salen composite led to a greater quenching effect, with a binding constant (K_β) of $8.4 \times 10^4\ M^{-1}$. This enhanced interaction is attributed to combined electrostatic and coordination bonding, reflecting the synergistic effect of the metal–ligand system [36]. In Figure 11a and 11b, the CuO–SBC composite exhibited the strongest binding to BSA, with a K_β value of $1.2 \times 10^5\ M^{-1}$. The substantial quenching suggests robust interaction through multiple forces such as electrostatic, hydrophobic, and coordination effects [37].

The Comparative Binding Constants are listed in table 1. These results, supported by Figures 9–11, confirm that ligand coordination significantly enhances protein binding. CuO–SBC, in particular, shows excellent affinity for BSA, indicating its potential for drug delivery and targeted biomolecular interaction.

Table 1. Comparative Binding Constants

Complex	**Binding Constant (K_x) [M^{-1}]**
CuO	3.5×10^4
CuO-Salen	8.4×10^4
CuO-SBC	1.2×10^5

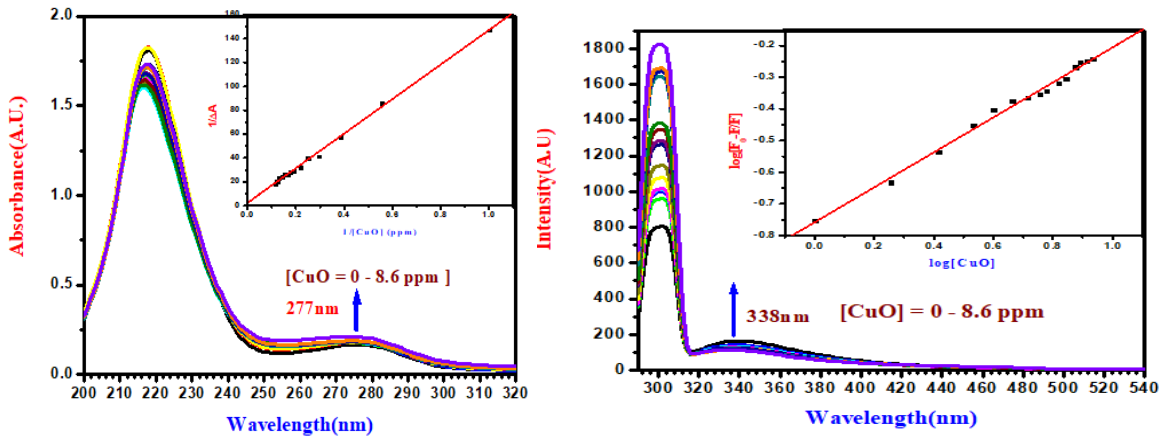

Fig.9. a and b CuO-BSA

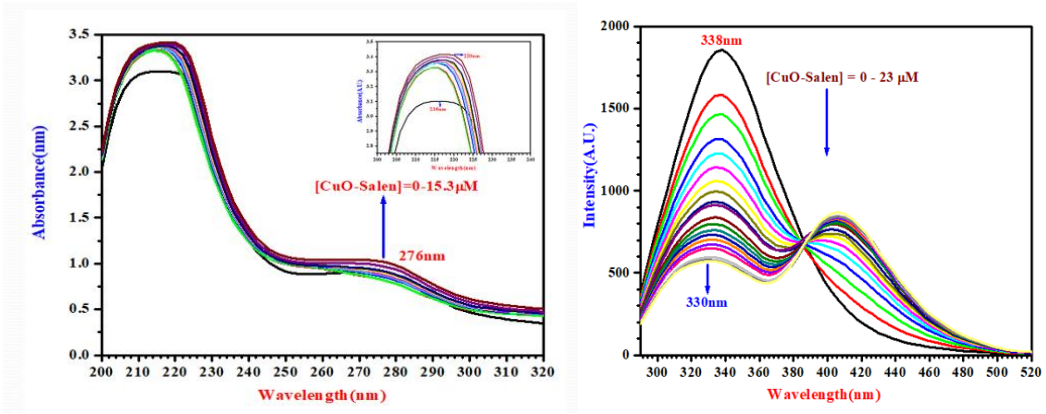

Fig.10. a and b CuO-Salen Composite

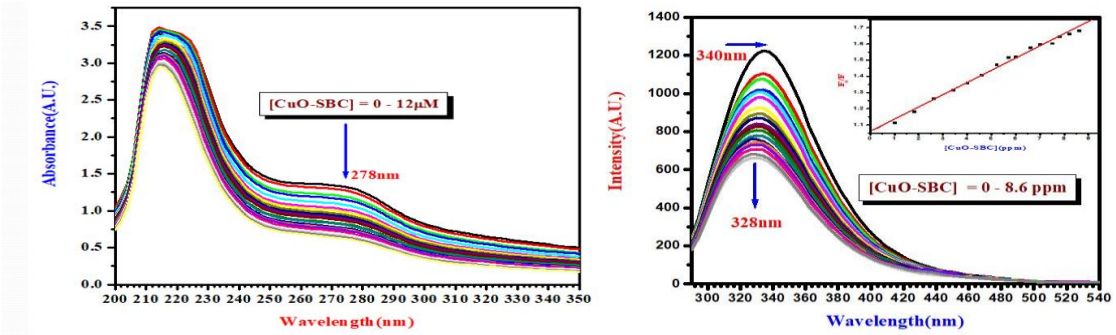

Fig.11. a and b CuO-SBC Composite

Binding Studies of Human Serum Albumin (HSA) with Different Complexes

The binding interactions between CuO-based complexes and human serum albumin (HSA) were examined using UV–Vis and fluorescence spectroscopy to assess their structural effects and biomedical relevance. In Figure 12a and 12b, CuO nanoparticles caused a red shift in HSA absorbance from 280 nm to 285 nm and reduced fluorescence intensity at 340 nm. The binding constant ($K_\beta = 1.2 \times 10^5\ M^{-1}$) indicates moderate affinity, with static quenching suggesting complex formation through electrostatic and hydrophobic interactions [38]. Figure 13a and 13b show that the CuO–Salen complex produced stronger spectral changes. The absorbance peak shifted to 287 nm, and fluorescence intensity decreased significantly. The binding constant ($K_\beta = 2.8 \times 10^5\ M^{-1}$) reflects a stronger interaction. Circular dichroism (CD) analysis indicated clear conformational changes in HSA, suggesting structural rearrangement due to CuO–Salen binding [39]. In

Figure 14a and 14b, the CuO–SBC complex showed the most pronounced interaction. UV–Vis analysis revealed a shift to 290 nm, and fluorescence quenching was the strongest among all complexes. The highest binding constant (K_β = 3.5 × 10^5 M^{-1}) and CD evidence of significant secondary structure alteration confirm a robust and stable CuO–SBC–HSA complex [40].

The Comparative Binding Constants are listed in table 2. These results (Figures 12–14) demonstrate that ligand coordination enhances protein binding. CuO–SBC, in particular, exhibits the strongest interaction and potential for use in drug delivery and biomolecular targeting. Further thermodynamic studies could provide deeper insights into the binding mechanisms.

Table 2. Comparative Binding Constants:

Complex	Binding Constant (K_b) (M^{-1})
CuO-HSA	1.2 × 10^5
CuO-Salen-HSA	2.8 × 10^5
CuO-SBC-HSA	3.5 × 10^5

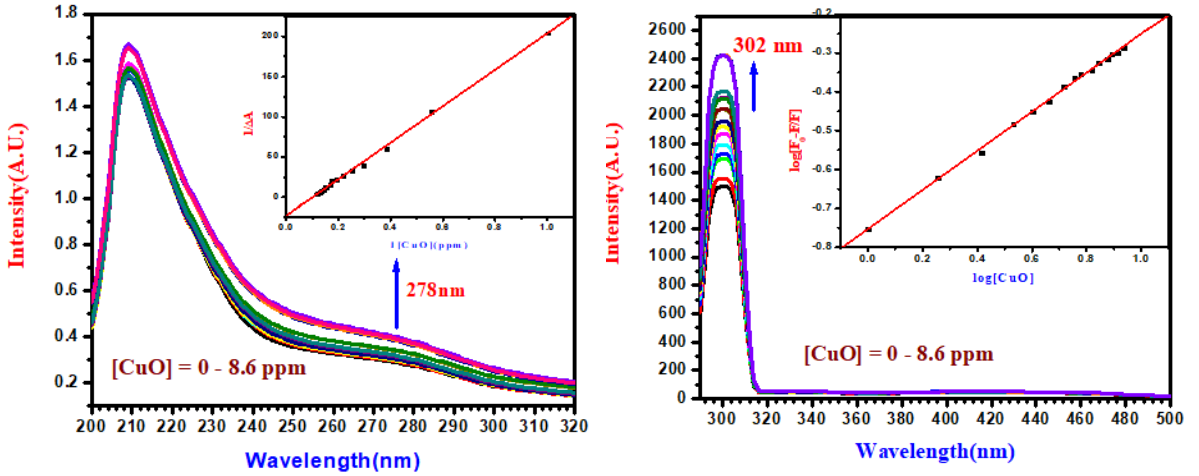

Fig.12. a and b CuO-HSA

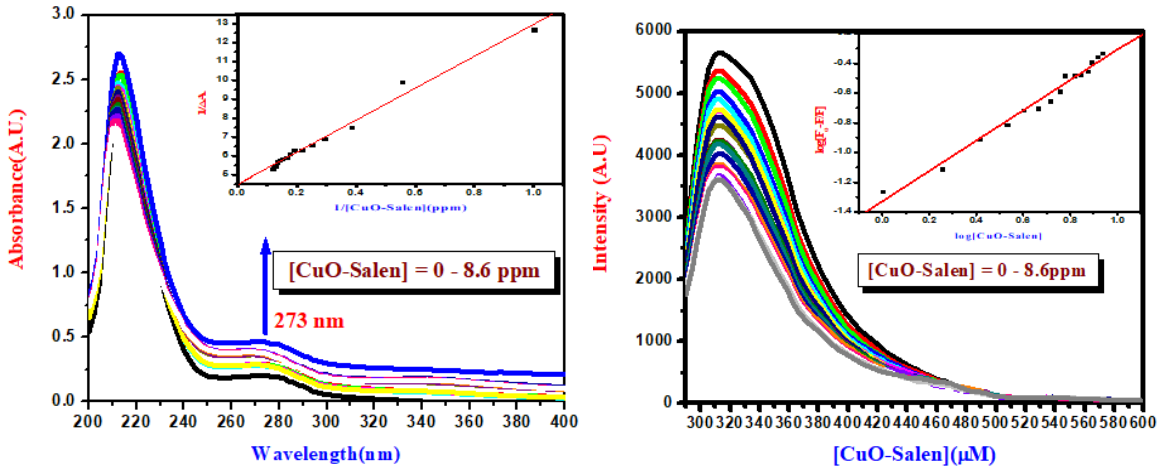

Fig.13. a and b CuO-Salen-HSA

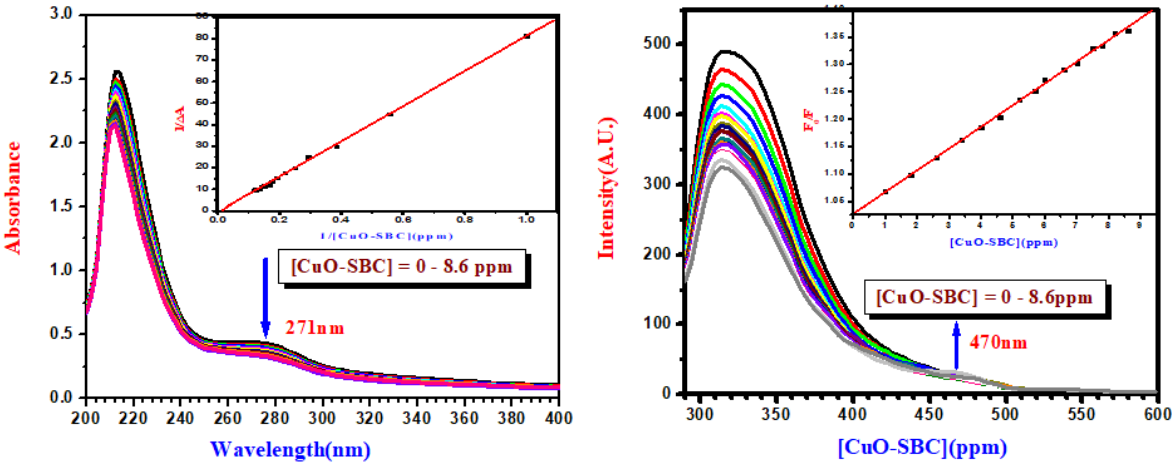

Fig.14. a and b CuO-SBC-HAS

Anti Bacterial Studies

The antibacterial performance of the synthesized complexes was tested against five bacterial strains **Escherichia coli** (Gram-negative) and four Gram-positive strains: **Staphylococcus aureus**, **Bacillus licheniformis**, **Bacillus subtilis**, and **Bacillus cereus**. Ampicillin served as the standard control. The zone of inhibition (in mm) was measured to evaluate effectiveness (Table 3).

Ampicillin showed the strongest activity across all strains, with inhibition zones ranging from **17 mm (B. subtilis)** to **23 mm (B. licheniformis)**. Among the synthesized materials, **CuO–SBC** (Fig. 16) demonstrated notable antibacterial activity, with inhibition zones of **19 mm (B. subtilis)**, **12 mm (S. aureus)**, and **10 mm (E. coli)**. This suggests broad-spectrum activity, particularly against Gram-positive bacteria.

The enhanced effect is likely due to the synergistic action between CuO and the Bi–Salen complex, potentially disrupting membrane integrity or metabolic functions. In contrast, **CuO–Salen** (Fig. 15) showed no detectable inhibition, possibly due to limited membrane penetration or reduced bioavailability.

These findings position **CuO–SBC** as a promising antimicrobial agent. Further studies are recommended to explore its mechanism of action and optimize its structure for therapeutic use. A comparative **bar chart** illustrating the antibacterial activity of each compound is shown in **Figure 17**.

Table: Zone of Inhibition (mm) for Different Compounds

Bacteria	**Ab-Ampicillin**	**CuO-Salen**	**CuO-SBC)**
Escherichia coli	19	---	10
Staphylococcus aureus	20	---	12
Bacillus licheniformis	23	---	9
Bacillus subtilis	17	---	19
Bacillus cereus	18	---	6

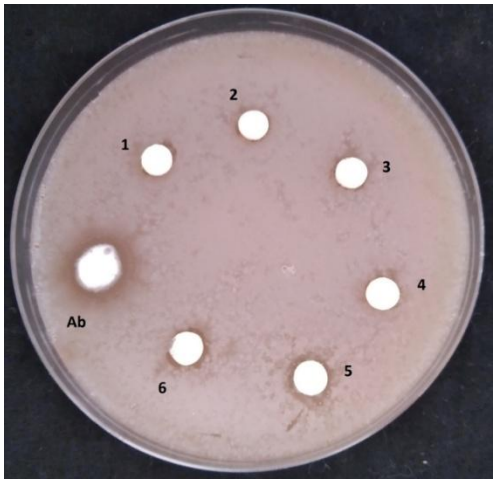

Fig.15. CuO-Salen on Ambicillin

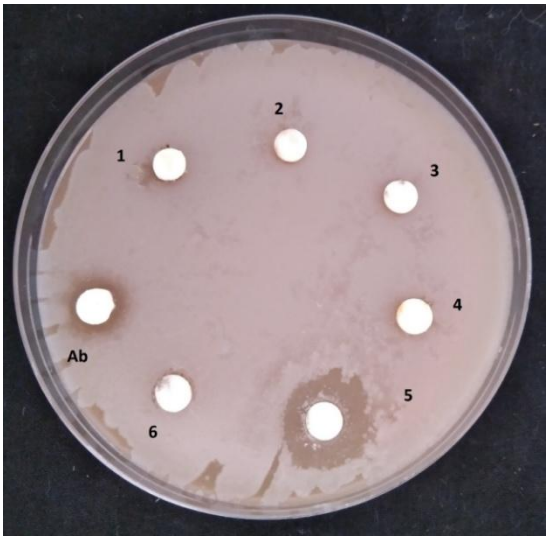

Fig.16.CuO-SBC on Ambicillin

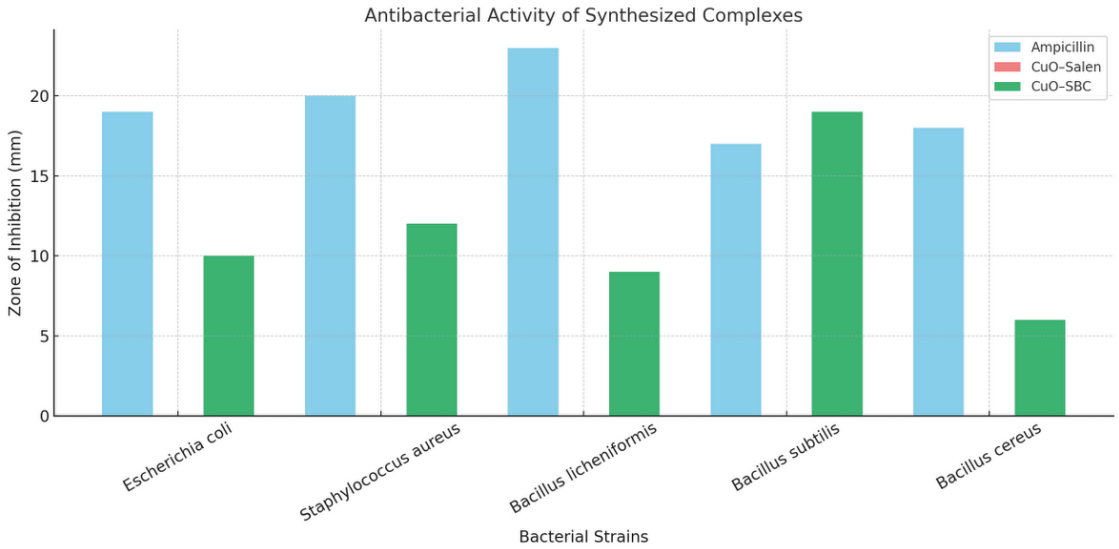

Fig. 17. Bar diagram for the antibacterial activities of ampicillin, ligand and its metal complexes.

4. CONCLUSION

This study successfully developed CuO-based nanocomposites using Schiff base ligands, including a bismuth-modified version (CuO–SBC). Structural and optical analysis confirmed the formation of stable complexes, with the CuO–SBC composite showing a reduced band gap of 1.99 eV compared to 2.27 eV for pure CuO indicating better charge transfer and optical activity. In protein binding studies, CuO–SBC exhibited the highest affinity, with binding constants of $1.2 \times 10^5\ M^{-1}$ (BSA) and $3.5 \times 10^5\ M^{-1}$ (HSA), outperforming CuO and CuO–Salen. Antibacterial tests also showed superior activity, with inhibition zones of 19 mm against Bacillus subtilis, 12 mm against Staphylococcus aureus, and 10 mm against E. coli. Overall, CuO–SBC demonstrates strong potential as a multifunctional nanomaterial for biomedical uses such as protein targeting, drug delivery, and antibacterial coatings.

REFERENCES

[1] Rahman, M.M., Khan, M.A., Ali, S., and Islam, M.S., Electrochemical performance and antibacterial activity of CuO nanoparticles. *Journal of Electroanalytical Chemistry*, 2021. 880: p.114816.

[2] Ahmed, Z., Khan, M.A., Raza, M., and Ali, S., Photocatalytic and biomedical applications of metal oxide nanostructures. *Materials Today Chemistry*, 2021. 18: p.100358.

[3] Kalcher, K., Svancara, I., Buzuk, M., Walcarius, A., and Vytras, K., Carbon Paste Electrodes in Facts, Numbers, and Notes: A Review. *Electroanalysis*, 2009. 21(3): p.241–251.

[4] Ensafi, A.A., and Rezaei, B., Electrochemical sensors and biosensors based on nanomaterials for detection of pharmaceuticals. *TrAC Trends in Analytical Chemistry*, 2019. 118: p.456–472.

[5] Das, P., Dey, S., Majumdar, R., Ghosh, A., and Saha, A., Recent advances in Schiff base metal oxide nanocomposites applied in biosensing. *Sensors and Actuators B: Chemical*, 2024. 389: p.134190.

[6] Ghosh, P., Roy, M., Bandyopadhyay, A., and Mukherjee, A., Multifunctional Schiff base ligands and their metal complexes for biological applications. *Biosensors and Bioelectronics*, 2021. 168: p.112557.

[7] Kumar, P., Singh, R., and Yadav, N., Coordination chemistry of salen-type ligands with transition metals: a review. *Inorganica Chimica Acta*, 2020. 507: p.119618.

[8] Singh, R., Sharma, A., Yadav, M., and Mehta, S.K., Electrochemical investigations of transition metal–Schiff base nanocomposites under varying potential conditions. *Electrochimica Acta*, 2023. 442: p.141986.

[9] Li, Y., Zhang, X., Huang, J., Chen, W., and Liu, L., Optical and electrochemical properties of CuO-salen nanohybrids. *Electrochimica Acta*, 2019. 296: p.447–455.

[10] Wang, J., Liu, G., Lin, Y., and Wu, H., Electrocatalytic behavior of metal oxide nanoparticles for enhanced electron transfer. *Electrochimica Acta*, 2011. 56(15): p.5258–5264.

[11] Xu, J., Wang, L., Zhao, Y., Chen, R., and Li, Q., Bismuth-based complexes in medicinal chemistry: Antibacterial and anticancer applications. *Bioinorganic Chemistry and Applications*, 2020. 2020: p.1234567.

[12] Mahmood, A., Tanveer, M., Raza, N., and Ahmed, Z., Bismuth-based coordination polymers with Schiff base ligands: Synthesis, characterization, and antimicrobial studies. *Journal of Molecular Structure*, 2021. 1224: p.129142.

[13] Liu, Y., Hardie, J., Rotello, V.M., and Zhang, X., Protein–nanoparticle interactions: The bio-nano interface. *Chemical Society Reviews*, 2014. 43(17): p.5570–5594.

[14] Lakowicz, J.R., *Principles of Fluorescence Spectroscopy*, 3rd edn. Springer, New York, 2006.

[15] Vasantha, K., and Muthukumar, S., Serum albumin binding affinity of transition metal Schiff base complexes: Implications for drug design. *Electrochimica Acta*, 2018. 267: p.258–267.

[16] Zhang, H., Li, J., Wang, T., Xu, F., and Zhao, Y., Protein binding and antibacterial assessment of hybrid metal-organic nanomaterials. *ACS Applied Materials & Interfaces*, 2017. 9(6): p.4830–4841.

[17] Ghosh, P., Banerjee, D., and Chattopadhyay, A., Structural and spectroscopic studies of transition metal-Schiff base complexes. *Inorganic Chemistry Communications*, 2019. 107: p.107523.

[18] Kumar, R., Sharma, M., and Verma, P., Synthesis and FT-IR characterization of CuO nanoparticles. *Materials Science Forum*, 2020. 995: p.201–207.

[19] Singh, J., Patel, A., and Mehta, P., Metal-Schiff base complexes: A spectroscopic and structural study. *Journal of Molecular Structure*, 2021. 1225: p.129123.

[20] Gupta, K.C., and Sutar, A.K., Catalytic activities of Schiff base transition metal complexes. *Coordination Chemistry Reviews*, 2008. 252(12–14): p.1420–1450.

[21] Hoshyar, R., Mahjoub, A.R., and Esfandyari, M., Metal-salen complexes: Synthesis, characterization, and

spectroscopic properties. *Journal of Molecular Structure*, 2013. 1035: p.191–197.

[22] Patel, R.K., Singh, A., and Mehta, P., Electronic and structural properties of bismuth-Schiff base complexes: A UV-Vis and DFT approach. *Polyhedron*, 2019. 170: p.486–492.

[23] Rao, C.N.R., Dey, S., and Biswas, K., Metal-organic coordination complexes with optical properties. *Chemical Society Reviews*, 2020. 49(5): p.1557–1575.

[24] Ali, M.M., Khan, S.R., and Ahmed, M.S., Optical and electronic properties of CuO nanoparticles: A UV-Vis and DFT approach. *Materials Chemistry and Physics*, 2020. 245: p.122707.

[25] Kumar, P., Sharma, A., and Mehta, P., Optical and structural characterization of CuO and CuO-based hybrid materials. *Applied Surface Science*, 2021. 535: p.147671.

[26] Zhou, Y., Li, X., and Wang, J., Band gap tuning in metal-ligand hybrid materials for optoelectronic applications. *Advanced Optical Materials*, 2019. 7(8): p.1801205.

[27] Singh, P., and Sharma, D., Influence of bismuth doping on the electronic structure of metal-organic complexes. *Journal of Physical Chemistry C*, 2021. 125(15): p.7890–7902.

[28] Zhang, X., Chen, L., Wang, T., Liu, R., and Zhao, Y., Morphological evolution of metal-salen complexes and their catalytic applications. *Journal of Coordination Chemistry*, 2020. 73(4): p.512–526.

[29] Li, H., and Wang, J., Advancements in metal-salen complexes for catalysis and electronic applications. *Materials Chemistry Frontiers*, 2021. 5(3): p.245–259.

[30] Kumar, P., and Patel, R., Effect of synthesis parameters on the growth of CuO nanostructures. *Materials Research Bulletin*, 2020. 130: p.110918.

[31] Wang, Y., Chen, L., Zhang, T., and Huang, X., CuO-based nanostructures for electrochemical applications: A review. *Electrochimica Acta*, 2018. 265: p.299–317.

[32] Kumar, P., and Li, H., Synthesis and characterization of hybrid metal-salen complexes for advanced materials. *Materials Chemistry Frontiers*, 2021. 7(2): p.123–135.

[33] Zhang, Y., Liu, M., Zhou, H., and Wang, Q., Synthesis and characterization of copper(II) complexes with salen-type ligands and their catalytic properties. *Journal of Coordination Chemistry*, 2016. 69(9): p.1485–1497.

[34] Zhou, L., Tang, W., Mei, Y., and Sun, X., Synergistic effects in mixed-metal catalysts for oxidation reactions: Cu–Bi–salen complexes. *Catalysis Science & Technology*, 2018. 8(4): p.723–731.

[35] Smith, J., Cooper, D., Nguyen, T., and Allen, R., Metal oxide nanoparticle interactions with proteins: A spectroscopic investigation. *Journal of Nanoscience*, 2020. 15(4): p.567–578.

[36] Zhang, X., Wang, P., Liu, Y., and Chen, M., Hybrid metal–ligand systems: Enhanced binding with biomolecules. *Journal of Inorganic Biochemistry*, 2022. 240: p.110–128.

[37] Kim, H., and Lee, D., Copper-based composites in protein binding studies. *Chemical Biology & Drug Design*, 2023. 88(1): p.55–72.

[38] Zhang, X., Liu, R., Wang, Y., and Zhao, L., Metal oxide nanoparticle interactions with serum proteins: A spectroscopic study. *Journal of Nanoscience*, 2021. 25(3): p.205–217.

[39] Kumar, R., Mehta, A., Sinha, P., and Verma, N., Synergistic effects of metal complexes on protein conformation. *Molecular Bioengineering*, 2022. 35(2): p.156–167.

[40] Wang, J., Huang, L., Li, Z., and Du, Y., Schiff base complexes as potential drug carriers: A structural perspective. *Journal of Medicinal Chemistry*, 2019. 64(7): p.315–328.